

HETEROCYCLES, Vol. 100, No. 3, 2020, pp. 440 - 449. © 2020 The Japan Institute of Heterocyclic Chemistry
Received, 24th January, 2020, Accepted, 17th February, 2020, Published online, 19th February, 2020
DOI: 10.3987/COM-20-14221

NEW SCHIFF BASES BASED ON 1-AMINOPYRIMIDIN-2-(1*H*)-ONE: DESIGN, SYNTHESIS, CHARACTERIZATION AND THEORETICAL CALCULATIONS

Zülbiye Kökbudak,^a Halime Güzin Aslan,^a and Senem Akkoç^{b*}

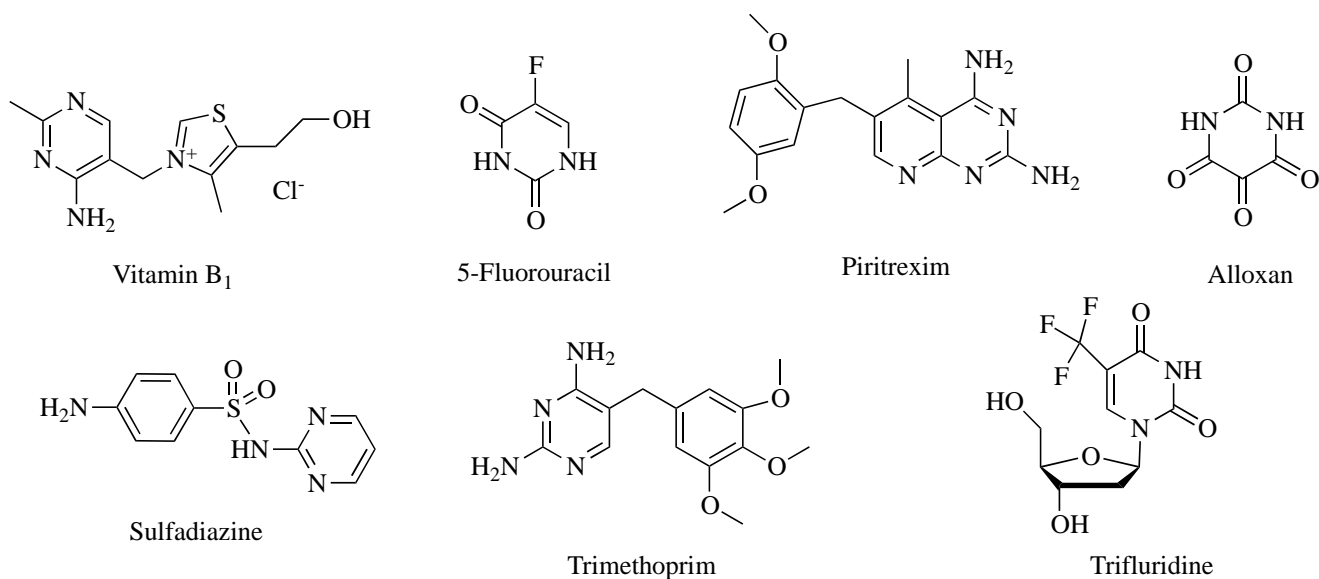
^aErciyes University, Faculty of Sciences, Department of Chemistry, 38000, Kayseri, Turkey. ^bSüleyman Demirel University, Faculty of Pharmacy, Department of Basic Pharmaceutical Sciences, 32260, Isparta, Turkey

Abstract – In this study, 1-amino-5-benzoyl-4-phenylpyrimidin-2(1*H*)-one (**1**) was synthesized from 4-benzoyl-5-phenylfuran-2,3-dione and 1-(1-phenylethylidene)semicarbazide in benzene. Since pyrimidine-based Schiff bases have an extensive working range, two new compounds (**2**, **3**) were synthesized from the reaction of this starting material (**1**) with 3-bromobenzaldehyde or 4-chlorobenzaldehyde. The structures of the synthesized new compounds were clarified employing FT-IR, ¹H NMR, ¹³C NMR, and elemental analysis. HOMO, LUMO, and energy gap between them was calculated as theoretical. On the other hand, conformation analysis studies of compounds were carried out for determining the energies of the conformers.

INTRODUCTION

Natural products having a pyrimidine ring system are important for the synthesis of agrochemical and pharmaceutical compounds.¹ A few natural products and some clinically used drugs having pyrimidine ring in their structures such as thiamine (vitamin B₁), 5-fluorouracil (an anticancer drug), piritrexim, sulfadiazine (an antibiotic), trimethoprim (an antibiotic), trifluridine (an antiviral drug) or alloxan are given in Scheme 1.

Pyrimidine based compounds have attracted the attention of researchers due to antiviral,² antibacterial,¹ antimicrobial,³ anticancer,⁴ antioxidant,⁵ diuretic,⁶ and antihistaminic⁷ activities. Furthermore, this type of compounds have catalytic activity properties, and they are used as a catalyst in different coupling reactions such as Mizoroki-Heck, Suzuki-Miyaura, Sonagashira, Negishi, arylation, etc.⁸



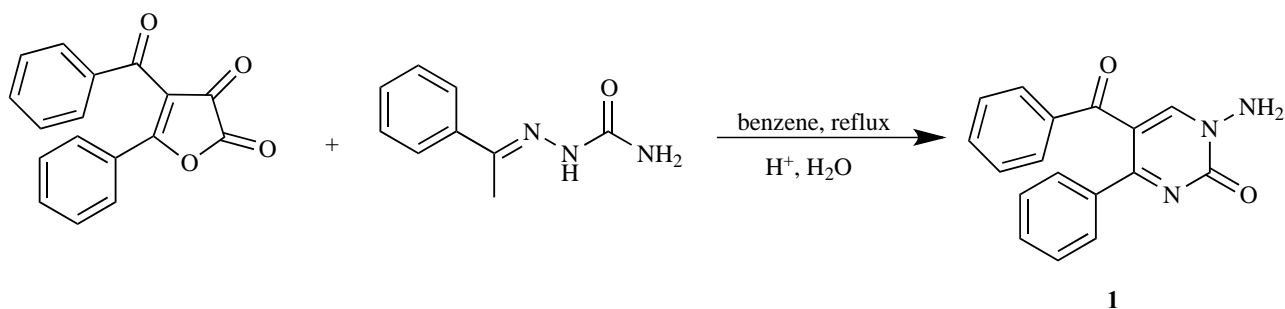
Scheme 1. Structures of a few known compounds bearing the pyrimidine nucleus

In the present study, two new compounds, namely 1-(3-bromobenzylideneamino)-5-benzoyl-4-phenylpyrimidin-2(1*H*)-one (**2**) and 1-(4-chlorobenzylideneamino)-5-benzoyl-4-phenylpyrimidin-2(1*H*)-one (**3**) were synthesized in two steps. Their structures were illuminated by spectroscopic and analytic methods. Moreover, the most stable conformers were optimized with the density functional theory (DFT/B3LYP) method in 6-311G(d,p) basis set. Conformation analysis of compounds was performed, and a few properties of these heterocyclic compounds were determined.

RESULTS AND DISCUSSION

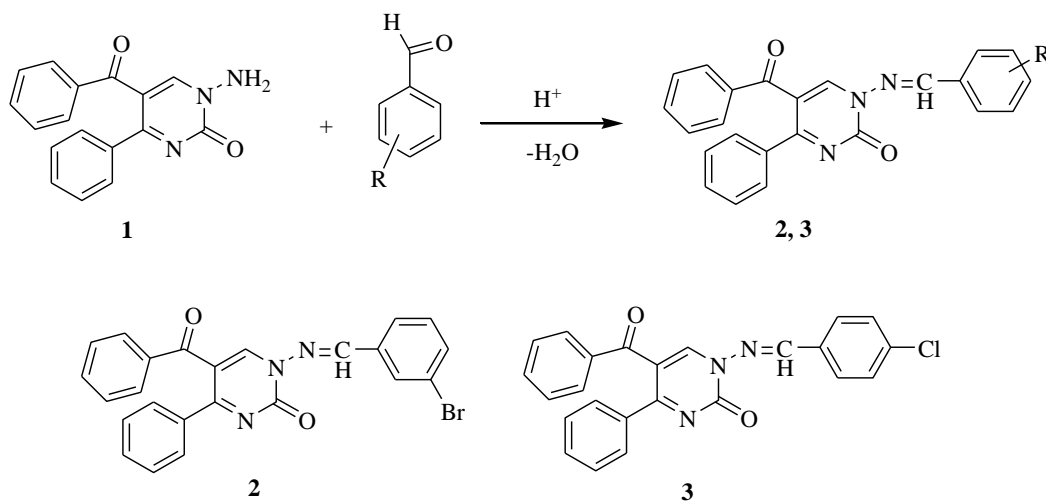
Pyrimidine compounds

Compound **1** was obtained from acetophenone semicarbazone with a furan-2,3-dione derivative (Scheme 2).



Scheme 2. Synthesis of compound **1**

Schiff bases as new compounds (**2** and **3**) were prepared from the reaction of 3-bromobenzaldehyde or 4-chlorobenzaldehyde with 1-amino-5-benzoyl-4-phenylpyrimidin-2(1*H*)-one (**1**) in high yields such as 77 and 73% for **2** and **3**, respectively (Scheme 3).



Scheme 3. Synthesis of compounds **2** and **3**

The IR spectrum of compounds demonstrated significant characteristic stretching bands to carbonyl (C=O) groups. These bands were observed at 1667.7 and 1649.5 cm^{-1} for **2**; 1683.8 and 1648.5 cm^{-1} for **3**. C=N stretching vibrations in Schiff bases were obtained as a sharp peak at 1619.8 and 1615.5 cm^{-1} for **2** and **3**, respectively. Aromatic C-H stretching vibrations were obtained at 3054.9 and 2893.9 cm^{-1} for **2**; 3050.3 and 3031.0 cm^{-1} for **3**. The presence of these characteristic functional groups such as C=O and C=N in IR supports the structures of the synthesized compounds (**2**, **3**).

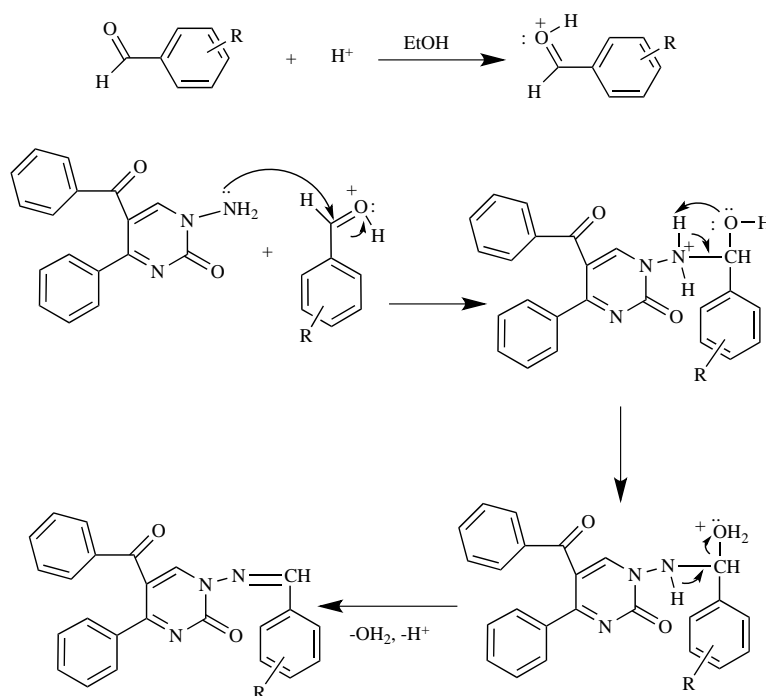
When ^1H NMR spectra of Schiff bases are examined, the most significant peak belongs to the azomethine proton, which is one of the characteristic peaks of such compounds. In the ^1H NMR spectrum, N=CH proton in the structure of compounds was resonated in the downfield area at δ 9.28 and 9.26 ppm for **2** and **3**, respectively. The proton signal belongs to the -CH in the pyrimidine ring was obtained as a singlet at δ 8.74 and 8.71 ppm for **2** and **3**, respectively. The aromatic protons of **2** and **3** were observed in between δ 8.13 and 7.32 ppm for **2**; in between δ 7.96 and 7.30 ppm as multiplet for **3**.

In ^{13}C NMR spectra, the signal of the benzoyl carbon was observed at δ 192.00 and 192.02 ppm for **2** and **3**, respectively. Other carbons of molecules were obtained in between δ 171.38 and 116.12 ppm. As a result, all data fully confirmed the structure of Schiff bases. Selected properties of compounds **2** and **3** are given in Table 1.

Table 1. A few characteristic data of **2** and **3**

Entry	Compounds	Yield (%)	Melting point (°C)	IR _(C=O) (cm ⁻¹)	Elemental analysis found (calc.)
1	2	77	222-223	1667.7, 1649.5	C: 62.65 (62.90); H: 3.40 (3.52); N: 9.01 (9.17).
2	3	73	171-172	1683.8, 1648.5	C: 69.50 (69.65); H: 3.75 (3.90); N: 9.59 (10.15).

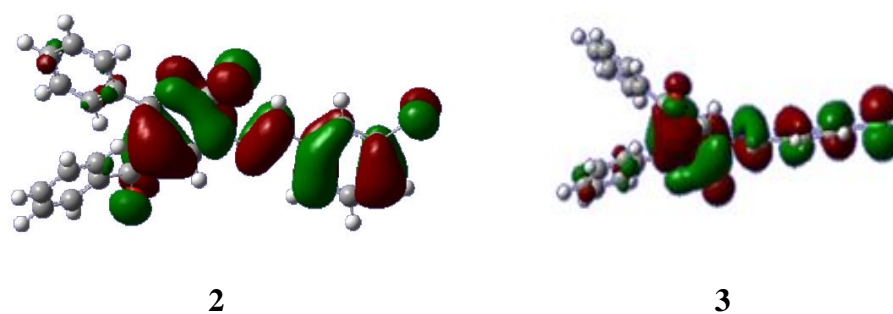
Schiff bases can be synthesized by different synthesis routes. Generally, the synthesis of Schiff bases from the reaction of primary amines with carbonyl compounds takes place as addition and elimination steps. First, a carbonyl amine intermediate is formed from the condensation of the amine and carbonyl group. Then, the Schiff base is obtained by the elimination of water. The mechanism of formation of synthesized Schiff bases (**2** and **3**) is shown in Scheme 4.



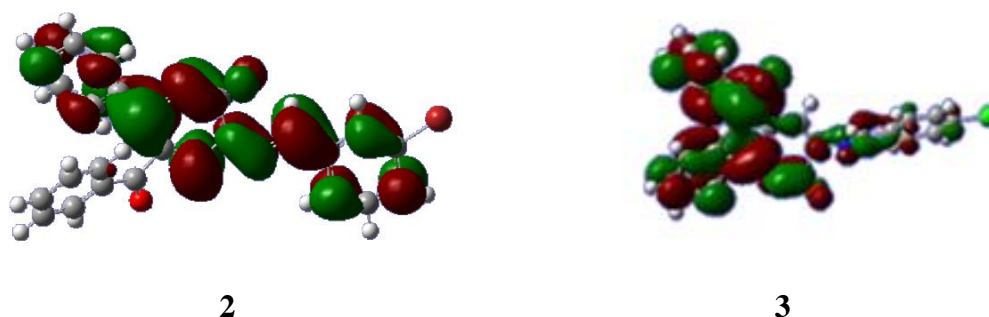
Scheme 4. The formation reaction mechanisms of targeted compounds

DFT studies

The theoretical calculations of **2** and **3** were done with the density functional theory (DFT/B3LYP) method in 6-311G(d,p) basis set. The highest occupied molecular orbital (HOMO) and the lowest unoccupied molecular orbital (LUMO) maps are given in Figures 1 and 2.

Figure 1. HOMO maps for **2** and **3**

The HOMO map of **2** shows that the surfaces were mostly situated over 3-bromobenzylideneamino (Figure 1). On the other hand, LUMO surfaces were settled over pyrimidine ring, 4-phenyl, and benzylideneamino (Figure 2).

Figure 2. LUMO maps for **2** and **3**

As can be seen in Figures 1 and 2, while HOMO surfaces were situated in the main over 4-chlorobenzylideneamino for **3**, LUMO surfaces were taken part in the pyrimidine ring, 4-phenyl, and benzylideneamino. A few electronic properties of compounds are given in Table 2.

Table 2. Electronic properties of **2** and **3**

Compounds	E_{HOMO} (eV)	E_{LUMO} (eV)	Electronegativity	Hardness
2	-0.0106	0.0491	0.14	0.19
3	-0.0283	0.026	0.14	0.19

The energy difference between LUMO and HOMO is called as energy gap and calculated with $\Delta E = E_{\text{LUMO}} - E_{\text{HOMO}}$ equation. According to this equation, the energy gap was found to be 0.0597 and 0.0543 eV for **2** and **3**, respectively. In general, molecules with a LUMO-HOMO gap of less than 1.5 eV are

chemically active.⁹ According to the calculated results, these two compounds are chemically active and kinetically stable.

Electrostatic potential maps of compounds

The MEP potential gives information about the electrostatic interactions applied by the total charge distribution of the molecule at a point in space. This value is directly related to the dipole moment, electronegativity, regional charge distribution, and chemical activity. Electrostatic potential maps give information about many properties such as size, load density, and chemical activity zones. Electrostatic potential values on the surface are expressed in different colors. Red color shows the highest electronegative charge (high electron density) area and demonstrates considerable solvent-solute interaction. Blue color characterizes the highest positive potential (low electron density) field and the fields suitable for nucleophilic attacks. Electrostatic potential maps of compounds **2** and **3** are given in Figure 3.

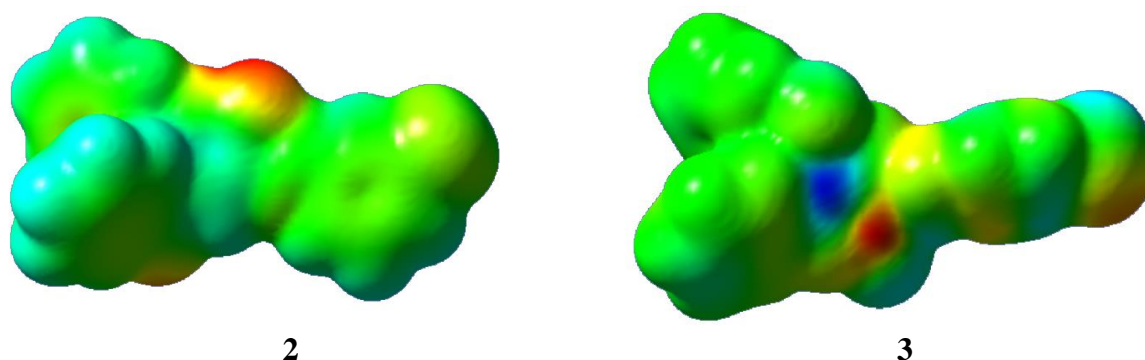


Figure 3. Electrostatic potential map of compounds **2** and **3**

The highest electron density in the molecules **2** and **3** are around the oxygen atom bound to the pyrimidine ring. This region is as a suitable site for chemical interaction. As a matter of fact, in the studies of complex synthesis with similar molecules, it was found that the ligand binds to the central atom via pyrimidine oxygen. The places shown in blue on the ESP map show areas with low electron density.

Conformation analysis studies

Rotations in molecules can occur around sigma bonds. There are two C = O and one N = C bonds in the structure of synthesized molecules. The benzene ring attached to the C = O group, pyrimidine ring, and imine carbon can rotate around the sigma bonds. The total number of conformers were determined. The Gaussian images of compounds **2** and **3** are given in Figure 4

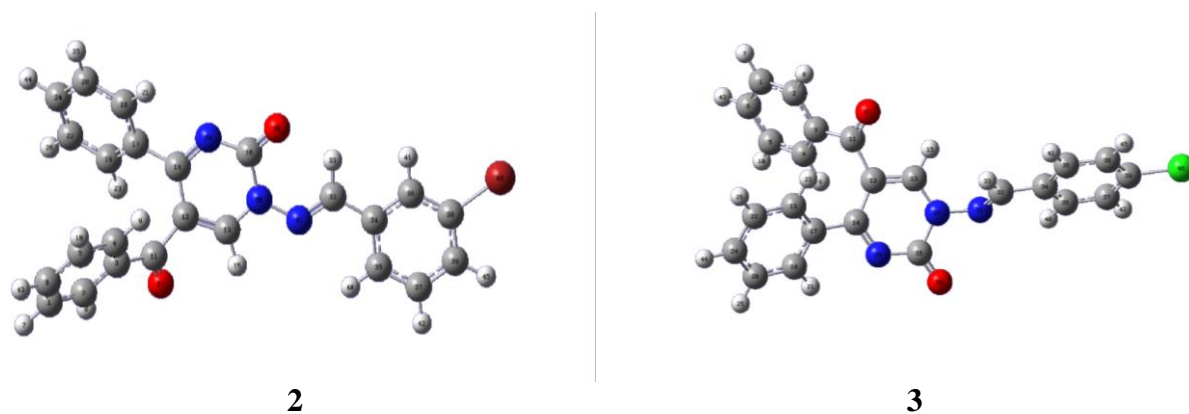
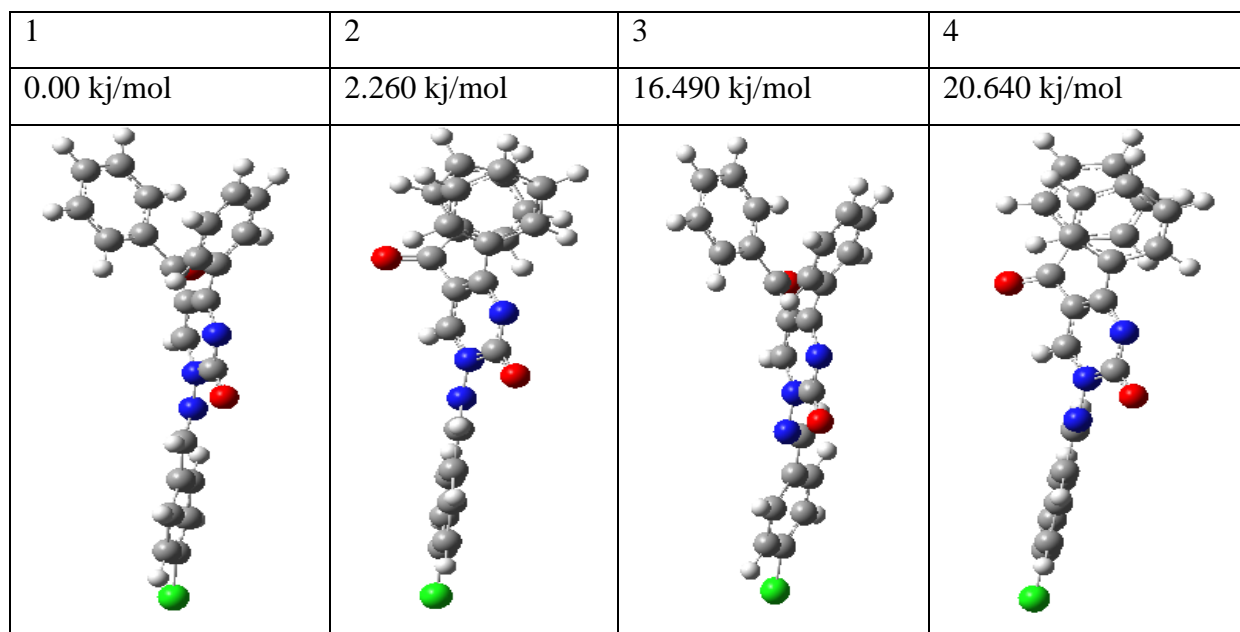


Figure 4. The optimized molecular structures of compounds **2** and **3** drawn by Gaussian software

The Gaussian images of the conformers of compounds **2** and **3** are shown in Figures 5 and 6, respectively. Compound **2** had seven conformers (Figure 5), and compound **3** had four conformers (Figure 6).

1	2	3	4	5	6	7
0.00 kj/mol	0.523 kj/mol	1.390 kj/mol	1.668 kj/mol	3.198 kj/mol	5.832 kj/mol	24.170 kj/mol

Figure 5. Conformers of compound **2**

Figure 6. Conformers of compound **3**

The synthesis of imine compounds (**2**, **3**) was realized in two steps as a result of the reaction of the starting arylamine and commercially available 3-bromobenzaldehyde or 4-chlorobenzaldehyde. Characterization of the new compounds **2** and **3** was done by ^1H NMR, ^{13}C NMR, FT-IR, and elemental analysis. The theoretical results show that the electronic densities of the molecules are concentrated on the pyrimidine ring and the benzene ring attached to the halogen. Furthermore, the calculated LUMO-HOMO gap values show that the chemical activity of the molecules is high.

EXPERIMENTAL

Instrumentation

The reagents and solvents used for the synthesis were purchased from different chemical companies. The melting point (mp) determination of compounds was recorded on the Electrothermal 9100 brand digital melting point device. The purities of the compounds were routinely monitored using DC Alufolien Kieselgel 60 F254-Merck thin layer chromatography and Camag brand TLC lamp (254/366 nm). Fourier Transform Infrared (FT-IR) spectra were obtained by Shimadzu Model 8400 FT-IR spectrophotometer. ^1H and ^{13}C NMR spectra were taken by Bruker brand 400 MHz (for ^1H NMR) and 100 MHz (for ^{13}C NMR) spectrophotometer. The conformational analysis of the molecules was performed with the density functional theory (DFT/B3LYP) method in 6-311G(d,p) basis set.

Synthesis of Schiff bases

0.1 mmol of compound **1** was dissolved in EtOH, and it was added to a solution of 0.1 mmol of 3-bromobenzaldehyde / 4-chlorobenzaldehyde in EtOH. It was refluxed for 40 min. It was then stirred for one day at room temperature. EtOH was removed from a rotary evaporator, and Et₂O was added instead of it. It was stirred in the cold for 24 h and then, was filtered. The solid obtained was crystallized three times with EtOH. The structures of the Schiff bases (**2** and **3**) were verified by ¹H NMR, ¹³C NMR, FT-IR, and elemental analysis.

1-(3-Bromobenzylideneamino)-5-benzoyl-4-phenylpyrimidin-2(1H)-one (2): Mixtures of compound **1** (1 mmol) and 3-bromobenzaldehyde (1 mmol) in 30 mL of EtOH were refluxed in the presence of a catalytic amount of *p*-toluenesulfonic acid as catalyst for 40 min. The solvent was evaporated after this reaction time. Then, the residue was treated with dry Et₂O and filtered. This Schiff base **2** obtained was purified with crystallization in EtOH. Yield: 0.35 g (77%); mp 222-223 °C; color: white. FT-IR: ν = 3054.9 and 2893.9 (C-H), 1667.7 and 1649.5 (C=O), 1619.8 and 1592.3 (C=C and C=N), 766-694 cm⁻¹ (pyr. ring). ¹H NMR (400 MHz, DMSO-*d*₆) δ (ppm) = 9.28 (s, 1H, N=CH), 8.74 (s, 1H, CH in pyrimidine ring), 8.13-7.32 (m, 14H, Ar-H). ¹³C NMR (100 MHz, DMSO-*d*₆) δ (ppm) = 192.00 (Ph-C=O), 171.38, 165.08, 151.50, 149.32, 137.24, 137.20, 135.76, 134.93, 133.96, 131.78, 131.40, 131.23, 130.22, 129.14, 128.72, 128.56, 122.75 and 116.21. Anal. Calcd for C₂₄H₁₆BrN₃O₂ (458.307 g/mol): C: 62.90; H: 3.52; N: 9.17. Found: C: 62.65; H: 3.40; N: 9.01.

1-(4-Chlorobenzylideneamino)-5-benzoyl-4-phenylpyrimidin-2(1H)-one (3): The reaction mixtures of compound **1** (1 mmol) and 4-chlorobenzaldehyde (1 mmol) in 30 mL of EtOH were refluxed in the presence of *p*-toluenesulfonic acid as catalyst for 40 min. After the solvent was evaporated, dry Et₂O was put on the product in a reaction flask and then filtered. The product **3** was recrystallized in EtOH. Yield: 0.30 g (73%); mp 171-172 °C; color: white. FT-IR: ν = 3050.3 and 3031.0 (aromatic C-H), 1683.8 and 1648.5 (C=O), 1615.5 and 1594.8 (C=N and C=C), 767-688 cm⁻¹ (pyr. ring skeleton). ¹H NMR (400 MHz, DMSO-*d*₆) δ (ppm) = 9.26 (s, 1H, N=CH), 8.71 (s, 1H, CH in pyridine ring), 7.96-7.30 (m, 14H, Ar-H). ¹³C NMR (100 MHz, DMSO-*d*₆) δ (ppm) = 192.02 (Ph-C=O), 171.28, 165.91, 151.50, 149.20, 137.96, 137.28, 137.22, 133.93, 131.46, 131.19, 131.09, 130.20, 129.80, 129.13, 129.09, 128.72 and 116.12. Anal. Calcd for C₂₄H₁₆ClN₃O₂ (413.856 g/mol): C: 69.65; H: 3.90; N: 10.15. Found: C: 69.50; H: 3.75; N: 9.59.

CONFLICT OF INTEREST

The authors have no conflict of interest to declare.

ACKNOWLEDGMENTS

We want to thank Erciyes University Research Fund (FBA-2019-8639) for their financial support.

SUPPORTING INFORMATION

<https://www.heterocycles.jp/newlibrary/downloads/PDFsi/26646/100/3>

REFERENCES

1. N. Kahriman, V. Serdaroğlu, K. Peker, A. Aydın, A. Usta, S. Fandaklı, and N. Yaylı, *Bioorg. Chem.*, 2019, **83**, 580.
2. S. Bai, S. Liu, Y. Zhu, and Q. Wu, *Tetrahedron Lett.*, 2018, **59**, 3179.
3. A. M. Fahim and A. M. Farag, *J. Mol. Struct.*, 2020, **1199**, 127025.
4. a) F. Yang, L.-Z. Yu, P.-C. Diao, X.-E. Jian, M.-F. Zhou, C.-S. Jiang, W.-W. You, W.-F. Ma, and P.-L. Zhao, *Bioorg. Chem.*, 2019, **92**, 103260; b) Z. Kökbudak, M. Saraçoğlu, S. Akkoç, Z. Çimen, M. İ. Yılmaz, and F. Kandemirli, *J. Mol. Struct.*, 2020, **1202**, 127261.
5. A. M. Farag and A. M. Fahim, *J. Mol. Struct.*, 2019, **1179**, 304.
6. A. Monge, V. Martinez-Merino, C. Sanmartin, F. J. Fernandez, M. C. Ochoa, C. Bellver, P. Artigas, and E. Fernandez-Alvarez, *Eur. J. Med. Chem.*, 1989, **24**, 209.
7. J. Quintela, C. Peinador, L. Botana, M. Estévez, and R. Riguera, *Bioorg. Med. Chem.*, 1997, **5**, 1543.
8. a) Y. Gök, S. Akkoç, M. Akkurt, and M. N. Tahir, *J. Iran. Chem. Soc.*, 2014, **11**, 1767; b) E. Fırıncı, *J. Mol. Struct.*, 2019, **1193**, 125; c) Z. Çimen, S. Akkoç, and Z. Kökbudak, *Heteroat. Chem.*, 2018, **29**, e21458; d) Y. Riadi, S. Lazar, and G. Guillaumet, *C. R. Chim.*, 2019, **22**, 294; e) M. Loubidi, A. Moutardier, J. F. Campos, and S. Berteina-Raboin, *Tetrahedron Lett.*, 2018, **59**, 1050; f) G. Aslan, S. Akkoç, M. Akkurt, N. Özdemir, and Z. Kökbudak, *J. Chin. Adv. Mater. Soc.*, 2018, **6**, 145; g) H. G. Aslan, S. Akkoç, Z. Kökbudak, and L. Aydın, *J. Iran. Chem. Soc.*, 2017, **14**, 2263.
9. a) B. Kesimli and A. Topaçlı, *Spectrochim. Acta, Part A.*, 2001, **57**, 1031; b) H. G. Aslan, *Suleyman Demirel Univ. J. Inst. Sci.*, 2017, **21**, 812.